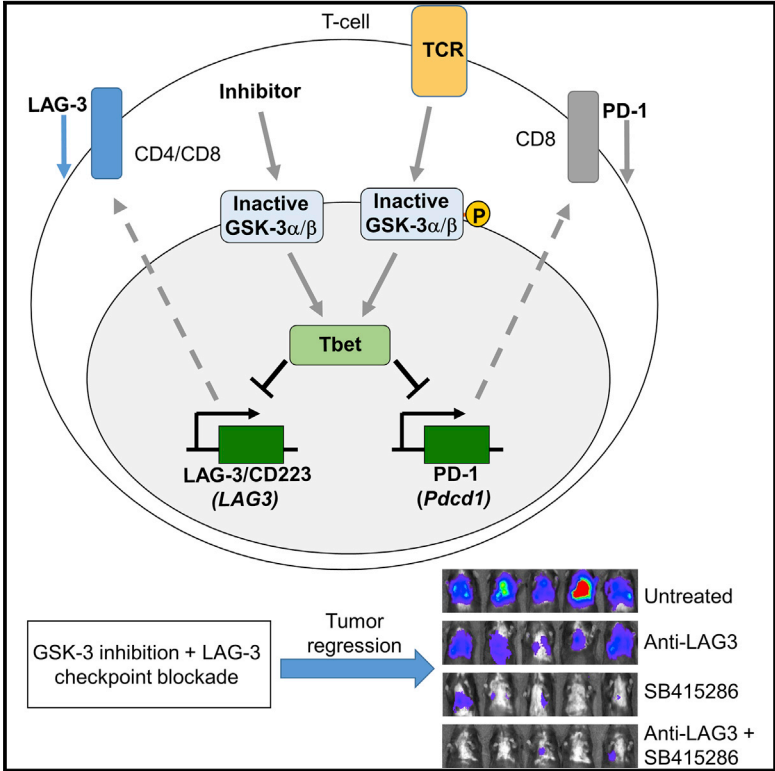# Cell Reports

Small Molecule Inhibition of GSK-3 Specifically Inhibits the Transcription of Inhibitory Co-receptor LAG-3 for Enhanced Anti-tumor Immunity

Graphical Abstract

Authors

Christopher E. Rudd, Kittiphat Chanthong, Alison Taylor

Correspondence

christopher.e.rudd@umontreal.ca (C.E.R.), a.tayor1@leeds.ac.uk (A.T.)

In Brief

Lymphocyte Activation Gene-3 (LAG-3) is a checkpoint molecule that has been targeted alongside programmed cell death (PD-1) for immunotherapy. Here, Rudd et al. demonstrate inhibition of glycogen synthase kinase-3 to control LAG-3 expression and that its combination with anti-LAG-3 antibody enhances T cell responses against tumors, causing tumor regression.

Highlights

- Glycogen synthase kinase-3 regulates the transcription of LAG-3 on CD4 and CD8 T cells

- Small molecule inhibitors (SMIs) of GSK-3 selectively downregulated LAG-3 and PD-1

- GSK-3 inhibition acted by upregulating the transcription factor Tbet

- Combining GSK-3 SMIs with anti-LAG-3 Ab is more effective than either alone

CellPress

Small Molecule Inhibition of GSK-3 Specifically Inhibits the Transcription of Inhibitory Co-receptor LAG-3 for Enhanced Anti-tumor Immunity

Christopher E. Rudd,[1,2,3,*] Kittiphat Chanthong,[1] and Alison Taylor[1,4,5,*]

[1]Cell Signalling Section, Department of Pathology, Tennis Court Road, University of Cambridge, Cambridge CB2 1QP, UK
[2]Division of Immunology-Oncology Research Center, Maisonneuve-Rosemont Hospital, Montreal, QC H1T 2M4, Canada
[3]Département de Medicine, Université de Montréal, Montreal, QC H3C 3J7, Canada
[4]Leeds Institute of Medical Research, University of Leeds, School of Medicine, Wellcome Trust Brenner Building, St James's University Hospital, Leeds LS9 7TF, UK
[5]Lead Contact
*Correspondence: christopher.e.rudd@umontreal.ca (C.E.R.), a.tayor1@leeds.ac.uk (A.T.)
 https://doi.org/10.1016/j.celrep.2020.01.076

SUMMARY

Immune checkpoint blockade using antibodies against negative co-receptors such as cytolytic T cell antigen-4 (CTLA-4) and programmed cell death-1 (PD-1) has seen much success treating cancer. However, most patients are still not cured, underscoring the need for improved treatments and the possible development of small molecule inhibitors (SMIs) for improved immunotherapy. We previously showed that glycogen synthase kinase (GSK)-3α/β is a central regulator of PD-1 expression, where GSK-3 inhibition down-regulates PD-1 and enhances CD8$^+$ cytolytic T cell (CTL) function, reducing viral infections and tumor growth. Here, we demonstrate that GSK-3 also negatively regulates Lymphocyte Activation Gene-3 (LAG-3) expression on CD4$^+$ and CD8$^+$ T cells. GSK-3 SMIs are more effective than LAG-3 blockade alone in suppressing B16 melanoma growth, while their combination resulted in enhanced tumor clearance. This was linked to increased expression of the transcription factor, Tbet, which bound the LAG-3 promoter, inhibiting its transcription, and to increased granzyme B and interferon-γ1 expression. Overall, we describe a small molecule approach to inhibit LAG-3, resulting in enhanced anti-tumor immunity.

INTRODUCTION

Immune checkpoint blockade (ICB) is a promising approach for the treatment of cancer. The approach involves the blockade of negative co-receptors on T cells such as cytolytic T cell antigen-4 (CTLA-4) and programmed cell death-1 (PD-1). PD-1 expression on tumor-infiltrating CD8$^+$ T cells correlates with impaired function (Ahmadzadeh et al., 2009), while PD-L1 expression on tumor cells facilitates their escape from the immune response (Iwai et al., 2002). ICB reverses T cell exhaustion and restores T cell function-

ality (Freeman et al., 2006; Wherry, 2011). The cancer treatment drug nivolumab (Opdivo) against PD-1 was approved as a first-line treatment for advanced melanoma and has been used alone, and in combination with ipilimumab (Yervoy), an anti-CTLA-4 antibody (Ab) resulting in high response rates (Hodi et al., 2010; Sharma et al., 2011; Wolchok et al., 2013). However, despite this success, many patients are still not cured and may suffer immune-related adverse events (irAEs). This poor prognosis continues to highlight a need to develop novel clinical interventions. In this context, we have identified the enzyme glycogen synthase kinase-3 (GSK-3) as a major nexus in the control of PD-1 expression on T cells (Taylor et al., 2016). We also showed that small molecule inhibitors (SMIs) of GSK-3 can suppress tumor growth in a manner comparable to PD-1 Ab blockade (Taylor et al., 2018).

Among the expanding numbers of inhibitory co-receptors on T cells are Lymphocyte Activation Gene-3 (LAG-3), T cell immunoreceptor with immunoglobulin (Ig) and ITIM domains (TIGIT), CD244 (2B4), T cell Ig and mucin-domain containing-3 (TIM-3), CD160, killer-cell lectin like receptor G1 (KLRG-1), and B and T lymphocyte attenuator (BTLA-4) (Baumeister et al., 2016). LAG-3 is an activation antigen that negatively regulates T cells (Workman et al., 2004; Workman and Vignali, 2003). It is a cell-surface molecule initially discovered on natural killer (NK) cells (Triebel et al., 1990) and then on activated T cells (Huard et al., 1994), B cells, and plasmacytoid dendritic cells (Workman et al., 2009). Furthermore, LAG-3 is a member of the Ig superfamily, containing four Ig loops, with structural homology to CD4. Unlike CD4, the membrane-distal IgG domain contains an extra loop region that appears important for binding to major histocompatibility complex class II (MHC class II) molecules (Triebel et al., 1990). Aside from MHC class II antigens, fibrinogen-like protein-1 is a major immune inhibitory ligand of LAG-3 (Wang et al., 2019). Studies in LAG-3 knockout mice have demonstrated an inhibitory role for LAG-3 in controlling both CD4 and CD8 T cell proliferation in vitro and in vivo (Workman et al., 2004). This negative effect on T cell function is exerted through a poorly understood but unique amino acid sequence (KIEELE) in the intracellular domain (Workman et al., 2002). Importantly, LAG-3 and PD-1 are co-expressed at high levels in tumor-infiltrating lymphocytes (TILs) from murine ovarian tumor and EG7-bearing mice, and blockade of both

molecules enhances CD8$^+$ effector T cell frequency and function, thus enhancing anti-tumor immunity (Andrews et al., 2017; Huang et al., 2015; Woo et al., 2012).

We originally demonstrated that the inhibition of serine/threonine kinase GSK-3 downregulates PD-1 expression, which enhances T cell responses against viral infections (Taylor et al., 2016, 2018). There are two ubiquitously expressed and highly conserved isoforms of GSK-3, GSK-3α and GSK-3β, which have shared and distinct substrates, as well as functional effects. Both forms have been implicated in processes ranging from glycogen metabolism to gene transcription, apoptosis, and microtubule stability. The notable aspect of GSK-3 is that it is constitutively active in resting T cells (Embi et al., 1980; Woodgett, 1990) and is inhibited by receptor-induced activation signals (Woodgett, 2001).

Our findings also showed that GSK-3 inhibition operated primarily via a reduction in PD-1 transcription on CD8$^+$ T cells (Taylor et al., 2016, 2018). We further showed that SMIs against GSK-3 are as effective as anti-PD-1 Abs in restricting B16 and EL-4 tumor growth in mice (Taylor et al., 2018). In this article, we demonstrate that GSK-3SMIs and siRNAs can also downregulate LAG-3 expression on T cells and that combination therapy of SMIs with LAG-3 can significantly enhance the clearance of tumors in mice.

RESULTS AND DISCUSSION

Small Molecule Inhibition of GSK-3 Downregulates PD-1 and LAG-3 in T Cells

We have previously shown that the inactivation of GSK-3α/β increases Tbet expression for the downregulation of PD-1 expression (Taylor et al., 2016, 2018; Taylor and Rudd, 2017). By contrast, we found no effects on the expression of other T cell receptors, including CD3, CD4, CD8, CD28, CTLA-4, CD44, CD62L, TIM-3, CD3, BTLA, NKG2D, CD122, IL-2Rα, CD25, CD69, FasL, and CD8 (Taylor et al., 2016). However, given that Tbet can regulate the expression of multiple genes (Lazarevic and Glimcher, 2011), we widened our survey of potential GSK-3 targets. Of particular interest was the expression of other inhibitory receptors (IRs). To this end, CD8$^+$ OT-1 T cells were stimulated with OVA$_{257-264}$ (SIINFEKL) peptide in the presence or absence of the GSK-3 SMI SB415286 over 7 days, during which samples were assessed for LAG-3 expression using flow cytometry and PCR analysis. As expected from previous work (Taylor et al., 2016, 2018; Taylor and Rudd, 2017), the OVA-induced upregulation of PD-1 was markedly reduced by the presence of the GSK-3 SMI. Surprisingly, the expression of LAG-3 was also downregulated by the presence of SMI, while the expression of other IRs such as CTLA-4, BTLA-4, and TIM-3 was unaffected (Figure 1A).

T cells isolated from wild-type C57BL/6 mice activated with anti-CD3 showed an increase in LAG-3 expression that was reduced by the presence of SB415286 (Figure 1B, left panel). As expected, the level of LAG-3 expression on anti-CD3-activated $Pdcd^{-/-}$ (PD-1-deficient) T cells was higher than seen on control T cells, consistent with the inhibitory effect of PD-1 on T cell activation. Nevertheless, SB415286 markedly reduced LAG-3 levels on anti-CD3-activated $Pdcd^{-/-}$ T cells (Figure 1B,

right panel). These data showed that GSK-3 inactivation downregulates LAG3 independent of PD-1 expression.

We next assessed whether the suppression of LAG-3 expression was mediated at the level of transcription of LAG-3 throughout the 7-day time course, as seen by use of real-time PCR (Figure 1C). The level and time course of the inhibition of LAG-3 transcription was similar to that of PD-1, while CTLA-4 transcription was unaffected.

Moreover, different ATP-competitive inhibitors SB415286, SB216763, and CHIR99021 had similar effects on both LAG-3 and PD-1 expression (Figure 1D). SB216763 has been reported to have a preference for the GSK-3α isoform, whereas CHIR99021 preferentially inhibits GSK-3β (Kaidanovich-Beilin and Eldar-Finkelman, 2006). SB415286 competitively inhibits both isoforms, with a preference for the β isoform (Coghlan et al., 2000). In all cases, LAG-3 and PD-1 transcription levels were reduced.

LAG-3 is also known for its role in regulating CD4$^+$ T cell function (Workman et al., 2002); therefore, the effect of SMI in CD4$^+$ T cells was investigated using OT-II transgenic mice. CD4$^+$ OT-II T cells were activated with OVA$_{323-339}$ (ISQAVHAAHAEINEAGR) peptide in the presence or absence of SMI for 7 days. Flow cytometry showed that GSK-3 inactivation reduced expression of LAG-3 on CD4$^+$ T cells (Figures S1A and S1B). Similarly, inhibition of GSK-3 decreased LAG-3 expression on NK cells (defined as CD3$^-$NKp46$^+$ cells) (Figure S1C). Overall, our findings identified LAG-3 as a novel target regulated by the inhibition of GSK-3 in CD4 and CD8$^+$ T cells.

Anti-LAG-3 Treatment Combined with GSK-3 SMIs *In Vitro* Enhances CD8$^+$ T Cell Cytolytic Responses

Given that anti-LAG-3 and GSK-3 SMI treatment would not be expected to block LAG-3, we next assessed whether they cooperate to enhance antigen-specific CD8$^+$ T cell cytolytic responses (Figure 2). CD8$^+$ OT-I T cells were stimulated with OVA$_{257-264}$ for 5 days in the presence of anti-LAG-3 Ab at different doses. After 5 days of activation, the killing of EL4 lymphoma target cells by cytolytic T cells (CTLs) using a lactate dehydrogenase (LDH) release detection assay. EL4 cells were pulsed with OVA peptide before the incubation to induce an antigen-specific response. Non-pulsed EL4 cells were used as a control for background killing. A trend was observed in which anti-LAG-3 increased killing; however, this did not achieve statistical significance (Figure 2A). By contrast, the addition of GSK-3 SMIs did increase *in vitro* OT-I killing, and the combination of GSK-3 SMIs and anti-LAG-3 increased the killing further at statistically significant levels (Figure 2B). This was seen over a range of target ratios and was generally better than the cooperativity seen with anti-PD-1 and anti-LAG-3 combination therapy. Together, these data show that under conditions in which anti-LAG-3 blockade alone has limited effects in unleashing T cell responses against tumors, the inhibition of GSK-3, while having an effect on its own, sensitizes T cells to be more responsive to tumor antigens.

A similar cooperativity was observed when small interfering RNAs (siRNAs) against the GSK-3α and GSK-3β isoforms were used to knock down (KD) expression (Figure 2C). Naive
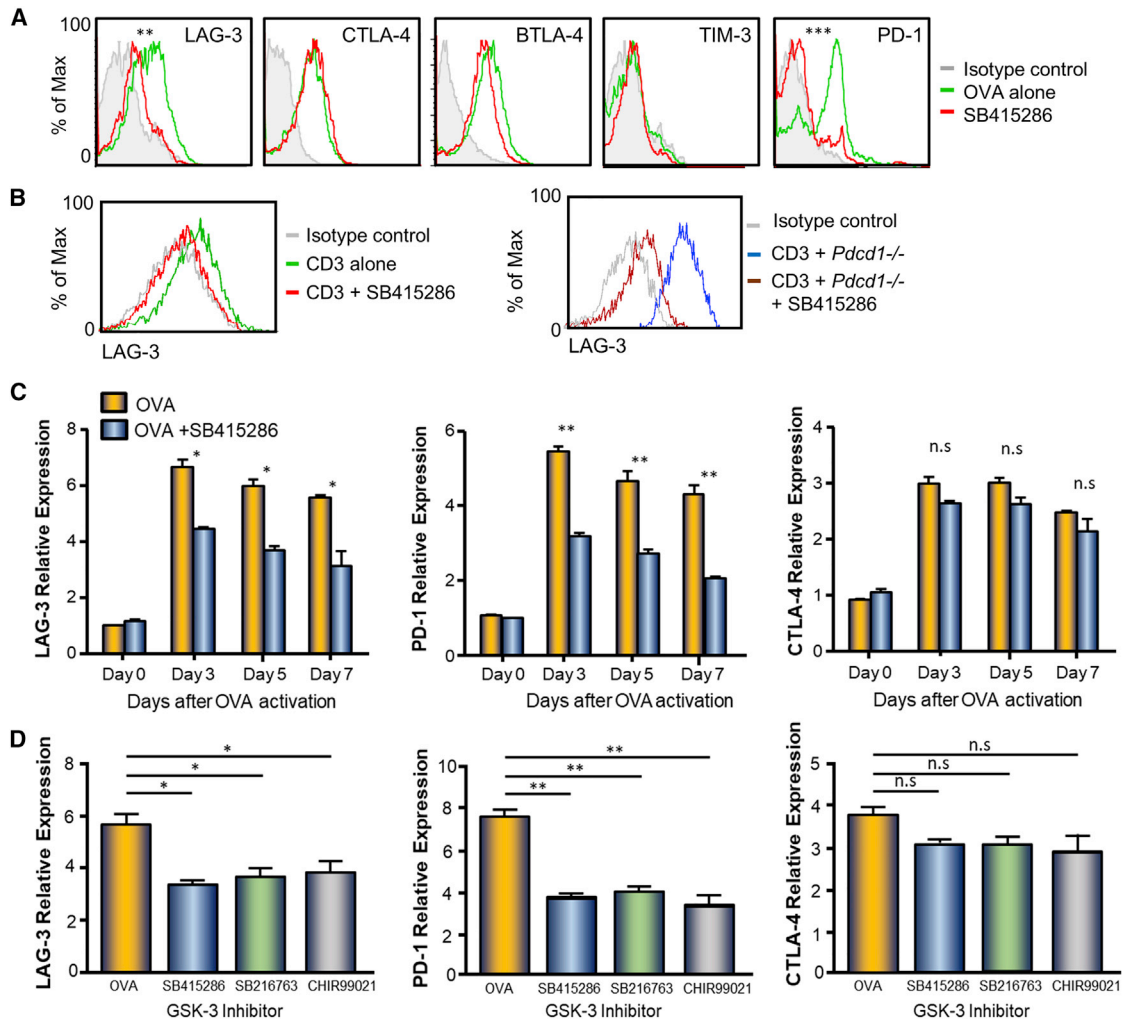
Figure 1. Inhibition of GSK-3 Downregulates PD-1 and LAG-3 on CD8+ T Cells

(A) OT-I CD8+ T cells stimulated with OVA peptide in the presence or absence of SB415286. Flow cytometric profiles. Green line, without SB415286; red line, with SB415286.

(B) C57BL/6 (left) or PD-1-deficient (right) T cells stimulated with anti-CD3 in the presence or absence of SB415286. Flow cytometric profiles. Green line, without SB415286; red line, with SB415286.

(C) Transcription of LAG-3 (left), PD-1 (middle), and CTLA-4 (right) in the presence or absence of SB415286.

(D) Downregulation of PD-1 and LAG-3 on OT-I CD8+ T cells in the presence of other GSK-3 inhibitors: SB216763 and CHIR99021.

Data are represented as mean ± SD based on triplicate values in individual experiments; data shown represent three independent experiments. Groups are compared using unpaired t test. *p < 0.05, **p < 0.01, ***p < 0.001. ns, not significant.

T cells were transfected before a 5-day activation period with OVA-pulsed EL4 cells and then assessed for cytolytic function using LDH release assays. siRNA treatment reduced GSK-3α and GSK-3β protein substantially, as seen by flow cytometry (Figure 2C, top panel), in which with the use of fluorescent GFP-conjugated siRNAs, more than 80% of cells took up the siRNAs. siRNAs to GSK-3 increased OT-I-mediated cytolysis of EL4-OVA targets when compared with the scrambled (Scrm) siRNA control (Figure 2C, bottom panel). This was significantly increased by the addition of anti-LAG-3 Ab. These data again showed that the combination of GSK-3 inactivation and anti-LAG-3 Ab therapy markedly increased the killing capacity of CD8+ OT-I CTLs.

Combined Treatment of Anti-LAG-3 Ab with GSK-3 SMIs *In Vivo* Enhances CD8+ T Cell Cytolytic Responses

To assess whether the combination of anti-LAG-3 with GSK-3 inhibition was effective in limiting tumor growth, B16 tumor cells tagged with luciferase were injected intravenously into C57BL/6 mice and treated with the GSK-3 SMI SB415286, anti-LAG-3, and/or anti-PD-1 (Figure 3). The optimal dose of SB415286, LAG-3, and PD-1 was established at 200 μg/mouse/treatment. SB415286 was administered every 2 days on six occasions, beginning 7 days post-injection of tumor cells, with the Ab given on four occasions (days 7, 10, 13, and 16). At days 10, 12, and 19, mice were injected intraperitoneally with luciferin and scanned by IVIS Lumina imaging (Figure 3A; Figure S2).
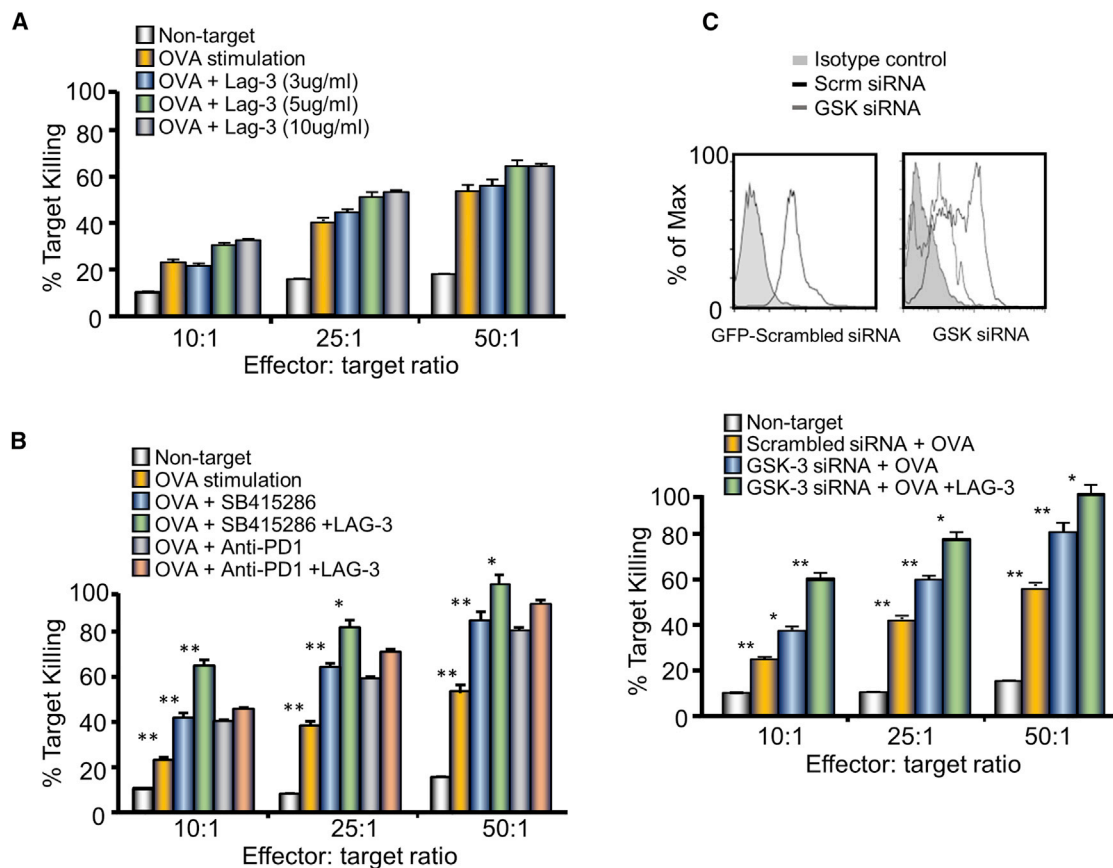
Figure 2. LAG-3 Potentiates the CD8$^+$ T Cell Cytolytic *In Vitro* Responses to GSK-3 Inhibition
(A) Cytolytic assay in response to OVA peptide in the presence of anti-LAG-3 at different concentrations.
(B) Cytolytic assay in response to GSK-3 inhibition combined with LAG-3 blockade.
(C) Flow cytometry profiles demonstrate siRNA uptake (upper left panel) using GFP-Scrm siRNA and KD of GSK-3 (gray line, upper right panel) in comparison to Scrm (black line). Cytolytic assay (lower panel) of GSK-3 siRNA-transfected OT-I cells in the presence or absence of LAG-3 blockade.
Statistical analysis based on triplicate values in individual experiments showing means and SDs (unpaired t test). *p < 0.05, **p < 0.01, ***p < 0.001.

Importantly, anti-LAG-3 treatment alone did not have a statistically significant effect on B16 tumor growth. Anti-PD-1 or SB415286 treatment alone reduced the luciferase signal relative to control at all time points. However, the combination of anti-LAG-3 with SB415286 treatment was seen to be the most effective in decreasing tumor growth. As reported (Huang et al., 2015; Zhang and Vignali, 2016), anti-LAG-3 plus anti-PD-1 also showed a trend in cooperating to reduce tumor size (Figure 3A); however, the combination of anti-LAG-3 and SB415286 was even more effective than anti-LAG-3 plus anti-PD-1. The efficacy of anti-LAG-3 with SB415286 treatment was observed by total flux measurements and the percentage of mice showing complete tumor clearance (Figure 3A, left panels). In both instances, the combination of anti-LAG-3 and GSK-3 inactivation was more effective than anti-LAG-3 plus anti-PD-1.

The cooperativity between anti-LAG-3 and SB415286 was particularly evident when we measured the complete loss of tumor (Figure 3A, right histogram). In this representative experiment, the combination was significantly more potent in clearing the tumor (3/5 mice) when compared with the effects

of anti-LAG-3 alone (0/5 mice) and SB415286 alone (1/5 mice). While the synergistic effects of PD-1 and LAG-3 on T cell function have been reported previously (Huang et al., 2015; Nguyen and Ohashi, 2015; Okazaki et al., 2011), our findings show that the combination of anti-LAG-3 plus GSK-3 inhibition is more effective than this previously documented combination against B16 melanoma. No direct effect of SB415286 on tumor cells was observed as previously demonstrated by treating B16 tumor-bearing Rag2−/− mice (devoid of B and T cells) with SB415286. Further, SB415286 had no obvious effect on tumor growth *in vitro* (Taylor et al., 2018).

The presence of SB415286 alone increased the presence of GZMB$^+$CD8$^+$CD3$^+$ T cells and TNF$^+$IFNγ^+CD3$^+$CD8$^+$ T cells (Figure 3B), while anti-LAG-3 alone also increased GZMB$^+$ T cells. However, the combination of anti-LAG-3 plus SB415286 or anti-LAG-3 plus PD-1 further increased the presence of TNF$^+$IFNγ^+CD3$^+$CD8$^+$ T cells and GZMB-expressing CD8$^+$CD3$^+$ TILs in accordance with the increased efficacy of tumor killing. The combination of anti-LAG-3 with SB415286 was generally more effective than anti-LAG-3 combined with anti-PD-1.
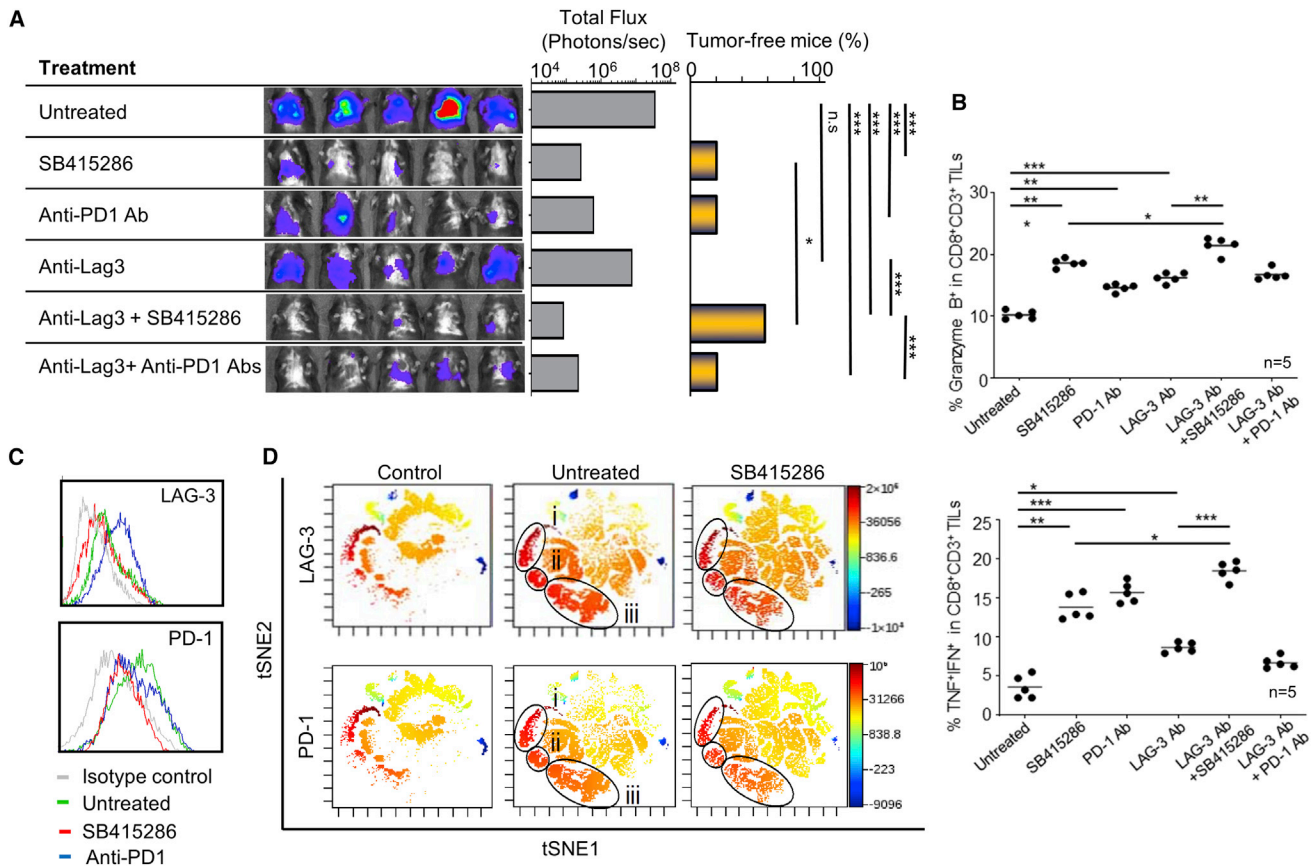
Figure 3. Combining GSK-3 Inhibition with Anti-LAG-3 Therapy Further Inhibits Pulmonary Metastasis of B16 Melanoma

(A) Luminescent image showing B16 metastasis at day 19 with total flux values (in photons per second) depicted in the histogram in the middle. The histogram on right shows the percentage of tumor-free animals at the end of the study on day 19 (n = 5).

(B) Anti-LAG-3 plus SB415286 increases the presence of granzyme B$^+$CD8$^+$CD3$^+$ TILs (upper panel) and TNF$^+$IFN$^+$CD8$^+$CD3$^+$ TILs (lower panel), as measured by flow cytometry (n = 5). GSK-3 inhibition of LAG-3 affects the PD-1$^+$ T cell subset.

(C) Flow cytometry analysis of TILs from B16 tumors showing the downregulation of LAG-3 and PD-1 (n = 5).

(D) viSNE profiles using CytoBank show that LAG-3 and PD-1 defined several overlapping populations of CD8$^+$ TILs. The three CD8$^+$ islands (i–iii) that were most brightly stained islands with anti-LAG-3 (upper panel) were also stained with anti-PD-1 (lower panel). TILs from mice treated with SB415286 showed reduced expression of LAG-3 on each of the three islands.

(A) Data shown from one individual experiment, representative of two independent experiments. (B) Represents two pooled experiments. Groups are compared using unpaired t test. *p < 0.05, **p < 0.01, ***p < 0.001. Data are represented as mean ± SEM.

Lastly, an examination of TILs showed that both LAG-3 and PD-1 on TILs were downregulated in this *in vivo* model (Figure 3C). Further analysis by CytoBank showed that anti-LAG-3 and PD-1 defined several overlapping populations of CD8$^+$ TILs (Figure 3D). Interestingly, the three CD8$^+$ islands (i–iii) that were the most brightly stained islands with anti-LAG-3 (upper panel) were also stained with anti-PD-1 (lower panel). TILs from mice treated with SB415286 showed a reduced expression of LAG-3 on each of the three islands. These data showed that three subpopulations of cells expressing LAG3 and PD-1 were affected by SB415286.

GSK-3 Downregulation or Inhibition Blocks LAG-3 Transcription

We have previously shown that inhibition of GSK-3 led to an increase in the transcription of *Tbx21* (encodes T-box transcription factor Tbet), which was inversely correlated with *Pdcd1* transcription (Taylor et al., 2016). We therefore examined whether the upregulation of Tbet due to GSK-3 inhibition was also connected to the downregulation of LAG-3. Mice were subjected to B16 melanoma and treated with, or without, SB415286. CD8$^+$ T cells were isolated from spleens harvested on day 19, and RT-PCR was performed (Figure 4A). Concurrent with the preceding findings, LAG-3 expression was reduced by the presence of SB415286. Furthermore, this was associated with an increase in *Tbx21* transcription. Chromatin immunoprecipitation (ChIP) with anti-Tbet Ab followed by RT-PCR confirmed that GSK-3 inhibition increased Tbet binding to the LAG-3 promoter in anti-CD3-activated primary T cells (Figure 4B).

We next examined whether GSK-3 mediated its effect on LAG-3 transcription via Tbet. OT-I CD8$^+$ T cells were transfected with either scrambled (Scrm) or Tbet siRNA (Figure 4C).
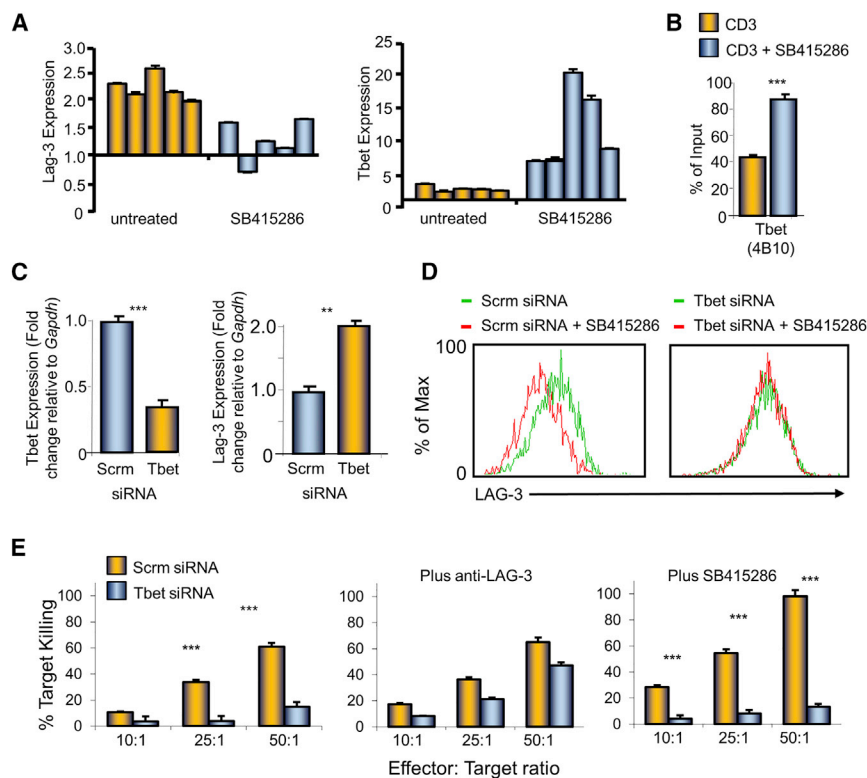
Figure 4. Inhibition of GSK-3 Inhibits LAG-3 and Increases Tbx21 Transcription

(A) *Tbx21* and LAG-3 transcription in response to B16 melanoma with or without SB415286 treatment.

(B) ChIP performed using CD3-activated primary T cells with or without SB415286. ChIP performed using anti-Tbet Ab followed by PCR analysis of LAG-3.

(C) Tbet siRNA used to block *Tbx21* transcription.

(D) Flow cytometry of LAG-3 expression on T cells expressing Scrm siRNA or Tbet siRNA in the presence or absence of SB415286.

(E) CTL killing efficiency of Tbet siRNA-expressing CTLs in the presence of anti-LAG-3 blockade or SB415286.

Statistical analysis based on triplicate values in individual experiments showing means and SDs (unpaired t test). *p < 0.05, **p < 0.01, ***p < 0.001.

Tbet siRNA expression decreased Tbet transcripts while increasing LAG-3 transcription, a result consistent with the negative regulation of LAG-3 by Tbet (Durham et al., 2014; Graydon et al., 2019; Kao et al., 2011). Importantly, SB415286 failed to reduce LAG-3 expression in cells expressing Tbet siRNA, as assessed by flow cytometry (Figure 4D). Tbet siRNA impaired CTL killing over different E:T ratios (Figure 4E). This inhibition was partially restored by LAG-3 blockade; however, GSK-3 inhibition had no effect. This result indicated that the modulatory effects of GSK-3 on LAG-3 expression operated in a pathway that required the expression of Tbet.

Overall, our findings demonstrating GSK-3 regulation of LAG-3 expression introduce a new pathway in the regulation of T cell responses in cancer immunotherapy. We have shown that GSK-3 now targets the two central IRs that are linked to T cell non-responsiveness or exhaustion (McLane et al., 2019; Wherry, 2011). Anti-PD-1 therapy, although effective, generates residual CD8+ T cells expressing PD-1+LAG-3+ T cells with an exhaustion phenotype (Wei et al., 2019). GSK-3 SMIs, by reducing the expression of both PD-1 and LAG3, should promote the functionality of T cells in tumors, either in the context of anti-PD-1 or LAG-3 immunotherapy. Future studies will assess whether the GSK-3-PD1/LAG3 axis also affects other key players like the transcription factor TOX in determining the response of intra-tumoral T-cells (Alfei et al., 2019). Importantly, our findings showed that the combination of anti-LAG-3 with GSK-3 inactivation was as effective as, or more effective than, anti-LAG-3 and anti-PD-1 in B16 melanoma cancer therapy. The synergic effect of LAG-3 with

PD-1 blockade has been studied extensively (Woo et al., 2012). One advantage of our approach in targeting GSK-3 involves the potential oral use of SMIs, which could be used in combination with anti-LAG-3. Intriguingly, in this context, we found that the combination of anti-LAG-3 plus SB415286 was more effective in the complete clearance of tumor mass than the combination of anti-LAG-3 and anti-PD-1. Its ability to compliment anti-LAG-3 presumably results from the limited effectiveness of Ab blockade in maintaining the complete blockade of receptors *in vivo*, as well as its ability to increase the expression of Tbet (Taylor et al., 2016), a key transcription factor for the development of CTLs and the transcription of granzymes and interferon-γ1 (Glimcher, 2007). Overall, our findings show that GSK-3 inactivation can potentiate the anti-tumor effects of anti-LAG-3 even more effectively than the combination anti-LAG-3 and PD-1 to eliminate tumor cells.

STAR★METHODS

Detailed methods are provided in the online version of this paper and include the following:

- KEY RESOURCES TABLE
- LEAD CONTACT AND MATERIALS AVAILABILITY
- EXPERIMENTAL MODEL AND SUBJECT DETAILS
  - Animals
  - Primary T cell cultures
  - Cell lines

- METHOD DETAILS
  - Generation of Cytolytic T cells
  - Activated CD4 T cells
  - Cytotoxicity Assays
  - Antibodies and reagents
  - Nuclear transfection
  - Flow cytometry
  - Quantitative real-time polymerase chain reaction (PCR)
  - Chromatin immunoprecipitation (ChIP) assay
  - Melanoma lung tumor establishment in wild-type mice
  - Isolation of tumor infiltrating lymphocytes (TILs)
- QUANTIFICATION AND STATISTICAL ANALYSIS
- DATA AND CODE AVAILABILITY

AUTHOR CONTRIBUTIONS

A.T. and C.E.R. designed the study. A.T. and K.C. conducted most experiments. A.T. and C.E.R. wrote the manuscript.

DECLARATION OF INTERESTS

The authors declare no competing interests.

REFERENCES

Ahmadzadeh, M., Johnson, L.A., Heemskerk, B., Wunderlich, J.R., Dudley, M.E., White, D.E., and Rosenberg, S.A. (2009). Tumor antigen-specific CD8 T cells infiltrating the tumor express high levels of PD-1 and are functionally impaired. Blood 114, 1537–1544.

Alfei, F., Kanev, K., Hofmann, M., Wu, M., Ghoneim, H.E., Roelli, P., Utzschneider, D.T., von Hoesslin, M., Cullen, J.G., Fan, Y., et al. (2019). TOX reinforces the phenotype and longevity of exhausted T cells in chronic viral infection. Nature 571, 265–269.

Andrews, L.P., Marciscano, A.E., Drake, C.G., and Vignali, D.A. (2017). LAG3 (CD223) as a cancer immunotherapy target. Immunol. Rev. 276, 80–96.

Baumeister, S.H., Freeman, G.J., Dranoff, G., and Sharpe, A.H. (2016). Coinhibitory Pathways in Immunotherapy for Cancer. Annu. Rev. Immunol. 34, 539–573.

Coghlan, M.P., Culbert, A.A., Cross, D.A., Corcoran, S.L., Yates, J.W., Pearce, N.J., Rausch, O.L., Murphy, G.J., Carter, P.S., Roxbee Cox, L., et al. (2000). Selective small molecule inhibitors of glycogen synthase kinase-3 modulate glycogen metabolism and gene transcription. Chem. Biol. 7, 793–803.

Durham, N.M., Nirschl, C.J., Jackson, C.M., Elias, J., Kochel, C.M., Anders, R.A., and Drake, C.G. (2014). Lymphocyte Activation Gene 3 (LAG-3) modulates the ability of CD4 T-cells to be suppressed in vivo. PLoS ONE 9, e109080.

Embi, N., Rylatt, D.B., and Cohen, P. (1980). Glycogen synthase kinase-3 from rabbit skeletal muscle. Separation from cyclic-AMP-dependent protein kinase and phosphorylase kinase. Eur. J. Biochem. 107, 519–527.

Freeman, G.J., Wherry, E.J., Ahmed, R., and Sharpe, A.H. (2006). Reinvigorating exhausted HIV-specific T cells via PD-1-PD-1 ligand blockade. J. Exp. Med. 203, 2223–2227.

Glimcher, L.H. (2007). Trawling for treasure: tales of T-bet. Nat. Immunol. 8, 448–450.

Graydon, C.G., Balasko, A.L., and Fowke, K.R. (2019). Roles, function and relevance of LAG3 in HIV infection. PLoS Pathog. 15, e1007429.

Hodi, F.S., O'Day, S.J., McDermott, D.F., Weber, R.W., Sosman, J.A., Haanen, J.B., Gonzalez, R., Robert, C., Schadendorf, D., Hassel, J.C., et al. (2010). Improved survival with ipilimumab in patients with metastatic melanoma. N. Engl. J. Med. 363, 711–723.

Huang, R.Y., Eppolito, C., Lele, S., Shrikant, P., Matsuzaki, J., and Odunsi, K. (2015). LAG3 and PD1 co-inhibitory molecules collaborate to limit CD8+ T cell signaling and dampen antitumor immunity in a murine ovarian cancer model. Oncotarget 6, 27359–27377.

Huard, B., Gaulard, P., Faure, F., Hercend, T., and Triebel, F. (1994). Cellular expression and tissue distribution of the human LAG-3-encoded protein, an MHC class II ligand. Immunogenetics 39, 213–217.

Iwai, Y., Ishida, M., Tanaka, Y., Okazaki, T., Honjo, T., and Minato, N. (2002). Involvement of PD-L1 on tumor cells in the escape from host immune system and tumor immunotherapy by PD-L1 blockade. Proc. Natl. Acad. Sci. USA 99, 12293–12297.

Kaidanovich-Beilin, O., and Eldar-Finkelman, H. (2006). Peptides targeting protein kinases: strategies and implications. Physiology (Bethesda) 21, 411–418.

Kao, C., Oestreich, K.J., Paley, M.A., Crawford, A., Angelosanto, J.M., Ali, M.A., Intlekofer, A.M., Boss, J.M., Reiner, S.L., Weinmann, A.S., and Wherry, E.J. (2011). Transcription factor T-bet represses expression of the inhibitory receptor PD-1 and sustains virus-specific CD8+ T cell responses during chronic infection. Nat. Immunol. 12, 663–671.

Lazarevic, V., and Glimcher, L.H. (2011). T-bet in disease. Nat. Immunol. 12, 597–606.

McLane, L.M., Abdel-Hakeem, M.S., and Wherry, E.J. (2019). CD8 T Cell Exhaustion During Chronic Viral Infection and Cancer. Annu. Rev. Immunol 26, 457–495.

Nguyen, L.T., and Ohashi, P.S. (2015). Clinical blockade of PD1 and LAG3—potential mechanisms of action. Nat. Rev. Immunol. 15, 45–56.

Okazaki, T., Okazaki, I.M., Wang, J., Sugiura, D., Nakaki, F., Yoshida, T., Kato, Y., Fagarasan, S., Muramatsu, M., Eto, T., et al. (2011). PD-1 and LAG-3 inhibitory co-receptors act synergistically to prevent autoimmunity in mice. J. Exp. Med. 208, 395–407.

Sharma, P., Wagner, K., Wolchok, J.D., and Allison, J.P. (2011). Novel cancer immunotherapy agents with survival benefit: recent successes and next steps. Nat. Rev. Cancer 11, 805–812.

Taylor, A., and Rudd, C.E. (2017). Glycogen Synthase Kinase 3 inactivation compensates for the lack of CD28 in the priming of CD8+ cytotoxic T-Cells: Implications for anti-PD-1 Immunotherapy. Front. Immunol. 8, 1653.

Taylor, A., Harker, J.A., Chanthong, K., Stevenson, P.G., Zuniga, E.I., and Rudd, C.E. (2016). Glycogen synthase kinase 3 inactivation drives T-bet-mediated downregulation of co-receptor PD-1 to enhance CD8(+) cytolytic T cell responses. Immunity 44, 274–286.

Taylor, A., Rothstein, D., and Rudd, C.E. (2018). Small-molecule inhibition of PD-1 transcription Is an effective alternative to antibody blockade in cancer therapy. Cancer Res. 78, 706–717.

Triebel, F., Jitsukawa, S., Baixeras, E., Roman-Roman, S., Genevee, C., Viegas-Pequignot, E., and Hercend, T. (1990). LAG-3, a novel lymphocyte activation gene closely related to CD4. J. Exp. Med. 171, 1393–1405.

Wang, J., Sanmamed, M.F., Datar, I., Su, T.T., Ji, L., Sun, J., Chen, L., Chen, Y., Zhu, G., Yin, W., et al. (2019). Fibrinogen-like Protein 1 Is a Major Immune Inhibitory Ligand of LAG-3. Cell *176*, 334–347.

Wei, S.C., Sharma, R., Anang, N.A.S., Levine, J.H., Zhao, Y., Mancuso, J.J., Setty, M., Sharma, P., Wang, J., Pe'er, D., and Allison, J.P. (2019). Negative Co-stimulation Constrains T Cell Differentiation by Imposing Boundaries on Possible Cell States. Immunity *50*, 1084–1098.

Wherry, E.J. (2011). T cell exhaustion. Nat. Immunol. *12*, 492–499.

Wolchok, J.D., Kluger, H., Callahan, M.K., Postow, M.A., Rizvi, N.A., Lesokhin, A.M., Segal, N.H., Ariyan, C.E., Gordon, R.A., Reed, K., et al. (2013). Nivolumab plus ipilimumab in advanced melanoma. N. Engl. J. Med. *369*, 122–133.

Woo, S.R., Turnis, M.E., Goldberg, M.V., Bankoti, J., Selby, M., Nirschl, C.J., Bettini, M.L., Gravano, D.M., Vogel, P., Liu, C.L., et al. (2012). Immune inhibitory molecules LAG-3 and PD-1 synergistically regulate T-cell function to promote tumoral immune escape. Cancer Res. *72*, 917–927.

Woodgett, J.R. (1990). Molecular cloning and expression of glycogen synthase kinase-3/factor A. EMBO J. *9*, 2431–2438.

Woodgett, J.R. (2001). Judging a protein by more than its name: GSK-3. Sci. STKE *2001*, re12.

Workman, C.J., and Vignali, D.A. (2003). The CD4-related molecule, LAG-3 (CD223), regulates the expansion of activated T cells. Eur. J. Immunol. *33*, 970–979.

Workman, C.J., Dugger, K.J., and Vignali, D.A. (2002). Cutting edge: molecular analysis of the negative regulatory function of lymphocyte activation gene-3. J. Immunol. *169*, 5392–5395.

Workman, C.J., Cauley, L.S., Kim, I.J., Blackman, M.A., Woodland, D.L., and Vignali, D.A. (2004). Lymphocyte activation gene-3 (CD223) regulates the size of the expanding T cell population following antigen activation *in vivo*. J. Immunol. *172*, 5450–5455.

Workman, C.J., Wang, Y., El Kasmi, K.C., Pardoll, D.M., Murray, P.J., Drake, C.G., and Vignali, D.A. (2009). LAG-3 regulates plasmacytoid dendritic cell homeostasis. J. Immunol. *182*, 1885–1891.

Zhang, Q., and Vignali, D.A. (2016). Co-stimulatory and Co-inhibitory Pathways in Autoimmunity. Immunity *44*, 1034–1051.

STAR★METHODS

KEY RESOURCES TABLE

REAGENT or RESOURCE	SOURCE	IDENTIFIER
Antibodies		
Anti-CD3 (2C11)	BioXCell	Cat# BE0001-1, RRID:AB_1107634
anti-PD-1 (CD279, J43)	BioXCell	Cat# BE0033-2, RRID:AB_1107747
anti-LAG-3 (C9B7W)	BioXCell	Cat# BE0174, RRID:AB_10949602
PD-L1 (E1L3N)	Cell Signaling Technology	Cat# 13684, RRID:AB_2687655
PE anti-human/mouse Granzyme B Recombinant Antibody	Biolegend	Cat# 372208, RRID:AB_2687032
PE/Cy7 anti-T-bet Antibody	Biolegend	Cat# 644824, RRID:AB_2561761
PE anti-mouse CD223 (LAG-3) Antibody	Biolegend	Cat# 125208, RRID:AB_2133343
APC anti-mouse CD279 (PD-1) Antibody	Biolegend	Cat# 135209
Alexa Fluor(R) 488 anti-mouse CD8a antibody	Biolegend	Cat# 100723, RRID:AB_389304
PE anti-mouse CD4 antibody	Biolegend	Cat# 100407, RRID:AB_312692
PE/Cy7 anti-mouse CD335 (NKp46) antibody	Biolegend	Cat# 137609, RRID:AB_10642684
Chemicals, Peptides, and Recombinant Proteins		
SB415286 3-(3-chloro-4-hydroxyphenylamino)-4-(2-nitrophenyl)-1H-pyrrole-2,5-dione	Abcam plc	Cat# ab120962
SB216763 3-(2,4-Dichlorophenyl)-4-(1-methyl-1H-indol-3-yl)-1H-pyrrole-2,5-dione	Abcam plc	Cat# ab120202
CHIR99021 6-[[2-[[4-(2,4-Dichlorophenyl)-5-(5-methyl-1H-imidazol-2-yl)-2-pyrimidinyl]amino]ethyl]amino]-3-pyridinecarbonitrile	Abcam plc	Cat# ab120890
OVA$_{257-264}$ peptide	Bachem	Cat# 4053142
OVA Peptide (323-339)	GenScript	Cat# RP10610
Critical Commercial Assays		
CytoTox 96® Non-Radioactive Cytotoxicity Assay	Promega	Cat# G1780
Pierce Agarose ChIP Kit	Thermo Scientific	Cat# 26156
RNeasy Mini kit	QIAGEN	Cat# 74104
TaqMan Reverse Transcription Reagents	Applied Biosystems	Cat# N808-0234
YBR® Green PCR Master Mix	Applied Biosystems	Cat# 4309155
Experimental Models: Cell Lines		
B16-F10-Luc2 (ATCC® CRL-6475-LUC2)	ATCC	Cat# CRL-6475-LUC2
EL4 (ATCC® TIB-39)	ATCC	TIB-39
Experimental Models: Organisms/Strains		
Mouse: OT II . C57BL/6-Tg(TcraTcrb)425Cbn/Crl	Charles River	https://www.criver.com/products-services/find-model/ot-ii-mouse
Mouse: OT I. C57BL/6-Tg(TcraTcrb)1100Mjb/Crl	Charles River	https://www.criver.com/products-services/find-model/ot-i-mouse
Oligonucleotides		
LAG-3-FW, 5′- CTACAACTCACCGCGTCATTT-3′;	Thermo Fisher Scientific	https://www.thermofisher.com/
LAG-3-RV, 5′-GCTCCAGACCCAGAACCTT-3′;	Thermo Fisher Scientific	https://www.thermofisher.com/
GAPDH-FW, 5-CAACAGCAACTCCCACTCTTC-3;	Thermo Fisher Scientific	https://www.thermofisher.com/
GAPDH- RW, 5- GGTCCAGGGTT TCTTACTCCTT-3	Thermo Fisher Scientific	https://www.thermofisher.com/
Tbet-FW, 5-GATCGTCCTGCAGTCTCTCC-3;	Thermo Fisher Scientific	https://www.thermofisher.com/
Tbet-RW, 5-AACTGTGTTCCCGAGGT GTC-3;	Thermo Fisher Scientific	https://www.thermofisher.com/
PD-1-FW, 5-CCGCCTTCTGTAATGGTTTGA-3;	Thermo Fisher Scientific	https://www.thermofisher.com/
PD-1-RV, 5-GGGCAGCTGTATGATCTGGAA-3;	Thermo Fisher Scientific	https://www.thermofisher.com/

(Continued on next page)

REAGENT or RESOURCE	SOURCE	IDENTIFIER
CTLA-4-FW, 5- ATG GCT TGC CTT GGA TTT CAG-3	Thermo Fisher Scientific	https://www.thermofisher.com/
CTLA-4 RW, 5- TCA ATT GAT GGG AAT AAA ATA-3	Thermo Fisher Scientific	https://www.thermofisher.com/
Software and Algorithms		
Prism	GraphPad	https://www.graphpad.com/ RRID:SCR_002798
FlowJo	BD	https://www.flowjo.com/solutions/flowjo
CytExpert	Beckman Coulter	https://www.mybeckman.uk/

LEAD CONTACT AND MATERIALS AVAILABILITY

Further information and requests for resources and reagents should be directed to and will be fulfilled by the Lead Contact, A.Taylor (a.taylor1@leeds.ac.uk). This study did not generate any new unique reagents.

EXPERIMENTAL MODEL AND SUBJECT DETAILS

Animals

C57BL/6, PD-1-deficient, OT-I and OT-II Tg mice were bred at the Department of Pathology, University of Cambridge. C57BL/6 were also bred at St James's Biomedical Service (SBS) unit, University of Leeds. 8-10 week old female mice were used for all analyses. Mice were housed in individually ventilated cages (IVC) and all experiments were approved by the Home Office UK (PPL No. 70/7544).

Primary T cell cultures

Spleen cells (taken from female mice – strains above) were treated with a hypotonic buffer with 0.15M NH4CL, 10mM KHCO3 and 0.1mM EDTA, pH 7.2 to eliminate red blood cells before suspension in RPMI 1640 medium supplemented with 10% FCS, 50uM beta-mercaptoethanol, sodium pyruvate, 2 mM L-glutamine, 100 U/ml penicillin and streptomycin (GIBCO). T cells were isolated from tumor and spleen samples, using T cell purification columns (R&D Systems).

Cell lines

B16F10 melanoma and EL4 lymphoma cells were cultured in DMEM medium supplemented with 10% FCS, 50uM beta-mercaptoethanol, sodium pyruvate, 2 mM L-glutamine, 100 U/ml penicillin and streptomycin (GIBCO).

METHOD DETAILS

Generation of Cytolytic T cells

OVA specific CD8$^+$ cytoytic T cells (CTLs) were generated by incubating isolated splenocytes OT-I mice with SIINFEKL peptide of OVA$_{257-264}$ peptide used at 10nM (Bachem Ag) for 5-7 days.

CTLs were generated in the presence or absence of inhibitors and/or anti-PD-1 or anti-Lag-3 for 5-7 days prior to washing and analysis by FACs, PCR or in cytotoxicity assays. GSK-3 inhibitors were reconstituted in DMSO to give a stock solution of 25mM and diluted to a concentration of 10uM for *in vitro* assays.

Activated CD4 T cells

OVA specific CD4+ T cells were generated by incubating isolated splenocytes from OT-II mice with SIINFEKL peptide of OVA$_{323-339}$ peptide used at 10nM (Bachem Ag) for 5-7 days in the presence or absence of SB415286.

Cytotoxicity Assays

Cytotoxicity was assayed using a Cytotox 96 non-radioactive kit (Promega) following the instructions provided. In brief, purified T cells were plated in 96-well plates at the effector/target ratios shown using 10^4 EL4 (pulsed with OVA peptide). Target cells per well were in a final volume of 200 μl per well using RPMI lacking phenol red. Lactate dehydrogenase release was assayed after 4 h incubation at 37°C by removal of 50 μl supernatant from each well and incubation with substrate provided for 30 min and the absorbance read at 490 nm using the Thermomax plate reader (Molecular Devices). Percentage cytotoxicity = ((experimental effectorspontaneous – target spontaneous)/(targetmaximum – target spontaneous)) x 100. All cytotoxicity assays were reproducible in at least three independent assays.

Antibodies and reagents

GSK3 inhibitors used at 10 μM *in vitro* and 200 μg/mouse *in vivo*; SB415286, SB216763 and CHIR99021 (Abcam plc). $OVA_{257-264}$ peptide used at 10nM (Bachem Ag).

Nuclear transfection

In certain cases, naive cells were subjected to nuclear transfection in the presence of various siRNA oligos (i.e., GSK-3). 3.0-5.0ug of siRNAs were added to 1×10^6 T cells and suspended in 100ul of Nucleofector^{TM} solution for T cells (Amaxa Biosystems, Cologne, Germany). Cells and oligos were then transferred into a cuvette and electroporated using program X-01 of the Nucleofector^{TM} (Amaxa Biosystems), and then immediately transferred into pre-warmed RPMI medium.

Flow cytometry

The following antibodies were used in experiments; Anti-CD3 (2C11), anti-PD-1 (CD279, J43) and anti-LAG-3 (C9B7W) (BioXCell); PD-L1 (E1L3N) (Cell Signaling Technology), conjugated antibodies anti-Granzyme B, anti-Tbet, anti-LAG-3 (C9B7W), CD279 (PD-1), anti-CD8α and anti-CD4 (Biolegend). Flow cytometry of antibody staining of surface receptors was conducted by suspending 10^6 cells in 100 μL PBS and adding antibody (1:100) for 2hr at 4°C. Cells were then washed twice in PBS. Cell staining was analyzed on a Beckman Coulter Cytoflex S and by CytExpert software. For intracellular staining, cells were fixed in 4% paraformaldehyde (PFA), permeabilized with 0.3% saponin (Sigma–Aldrich) and stained with the desired antibody in saponin containing PBS for 2hr at 4°C.

Quantitative real-time polymerase chain reaction (PCR)

RNA was isolated using an RNAeasy mini kit (QIAGEN) according to the manufacturer's instructions. Reverse transcription was performed to generate cDNA using TaqMan Reverse Transcription Reagents (Applied Biosystems). Quantitative real-time PCR used SYBR green technology (Applied Biosystems) on cDNA generated from the reverse transcription of purified RNA. After preamplification (95°C for 2 min), the PCRs were amplified for 40 cycles (95°C for 15 s and 60°C for 60 s) in a sequence detection system (PE Prism 7000; Perkin-Elmer Applied Biosystems). The exponential phase, linear phase and plateau phase of PCR amplification were carefully monitored to ensure a measurement of real time transcription. Data obtained was normalized against GAPDH expression using the standard curve method.

    LAG-3-FW, 5′- CTACAACTCACCGCGTCATTT-3′;
    LAG-3-RV, 5′-GCTCCAGACCCAGAACCTT-3′;
    PD-1-FW, 5-CCGCCTTCTGTAATGGTTTGA-3;
    PD-1-RV, 5-GGGCAGCTGTATGATCTGGAA-3;
    GAPDH-FW, 5-CAACAGCAACTCCCACTCTTC-3;
    GAPDH- RW, 5- GGTCCAGGGTT TCTTACTCCTT-3
    CTLA-4-FW, 5- ATG GCT TGC CTT GGA TTT CAG-3
    CTLA-4 RW, 5- TCA ATT GAT GGG AAT AAA ATA-3
    Tbet-FW, 5-GATCGTCCTGCAGTCTCTCC-3
    Tbet-RW, 5-AACTGTGTTCCCGAGGT GTC-3

Chromatin immunoprecipitation (ChIP) assay

C57BL/6 primary T cells were purified using CD3$^+$ T cell enrichment columns, 3×10^6 cells were used as a resting (input) control while remaining cells were cultured with anti-CD3 with/without SB415286 for 72h. Chromatin was prepared from all samples (3×10^6 cells) and used for ChIP assay following the manufacturers protocols - Pierce^{TM} Agarose ChIP kit (Thermo Scientific). Chromatin samples were immunoprecipitated with antibodies to Tbet, LAG-3, a positive control (anti-RNA polymerase II), or a negative control Rabbit Ig, both of the latter being provided in the kit. The resulting purified DNA with bound Ab was then quantified by RT-PCR. The results were normalized to the non-specific antibody control as well as a standardized aliquot of the input chromatin.

Melanoma lung tumor establishment in wild-type mice

B16 melanoma cells (2×10^5 taken from the log phase of *in vitro* growth) tagged with luciferase were transferred intravenously into syngeneic C57BL/6 mice 8-10 weeks old.

Treatment with SB415286 (200 μg/mouse) was given on days 7, 9, 11, 13, 15 and 17 post infection. Anti-LAG-3 (200 μg/mouse) and/or anti-PD-1 (200 μg/mouse) treatment was given on days 7, 10, 13 and 16.

Live imaging was performed at the time points indicated. Mice were injected intraperitoneally with luciferin (2 ug per mouse), anaesthetized with isoflurane and scanned with an IVIS Lumina (Caliper Life Sciences). For quantitative comparisons, we used Living Image software (Caliper Life Sciences) to obtain the maximum radiance (photons per s per cm2 per steradian, i.e., photons s−1 cm−2 sr−1) over each region of interest, relative to a negative control region. The lungs were excised 19 days after initial transfer.

Isolation of tumor infiltrating lymphocytes (TILs)

Lungs were harvested from mice at the time indicated. Tissue was disrupted using a blade and then incubated in HBSS solution containing 200units/ml of collagenase at 37°C for 2 hr. Tissue was then passed through a strainer and cells collected and layered onto ficoll before centrifugation. Tumor infiltrating cells were then collected from the lymphocyte layer.

QUANTIFICATION AND STATISTICAL ANALYSIS

The mean and SE of each treatment group were calculated for all experiments. The number of samples is indicated in the figure legends. Unpaired Student's t tests or ANOVA tests were performed using the InStat 3.0 software (GraphPad). In certain instances, statistics were done using 2-way ANOVA, or by non-parametric Mann Whitney at each time point. * $p < 0.05$, ** $p < 0.01$, *** $p < 0.001$.

DATA AND CODE AVAILABILITY

This study did not generate/analyze datasets/code